Journal of The Electrochemical Society, **155** (3) B232-B235 (2008)
0013-4651/2008/155(3)/B232/4/$23.00 © The Electrochemical Society

Characteristics and Performance of Electrolyte-Supported Solid Oxide Fuel Cells under Ethanol and Hydrogen

R. Muccillo,[a,*] E. N. S. Muccillo,[a,*] F. C. Fonseca,[a] and D. Z. de Florio[b,z]

[a]*Instituto de Pesquisas Energéticas e Nucleares, 05508-000, São Paulo, SP, Brazil*
[b]*Universidade Federal do ABC, 09210-170, Santo André, SP, Brazil*

A direct ethanol solid oxide fuel cell (SOFC) fabricated from conventional materials is described. The performance of Ni-cermet anodes with zirconia and ceria as the ceramic phase in SOFCs operating on hydrogen and ethanol is compared by means of current-voltage and impedance spectroscopy measurements in the 700–900°C temperature range. The experimental data indicate that the studied ethanol-fueled SOFCs have comparable performance. However, different ceramic matrix and metallic phase composition of cermets result in different behavior of the ethanol direct oxidation. Below 800°C, the performance of fuel cells is relatively more stable as compared to higher temperatures, but the catalytic activity for ethanol conversion of doped ceria is insufficient to prevent carbon formation. The experimental results provide evidence for the importance of an appropriate combination of fuel, operating conditions, and anode materials in designing SOFCs for direct operation using ethanol as fuel.
 [DOI: 10.1149/1.2828024]

Manuscript submitted September 11, 2007; revised manuscript received November 29, 2007.
Available electronically January 9, 2008.

Fuel cells have been increasingly accepted as efficient energy conversion systems with low environmental impact. In particular, solid oxide fuel cells (SOFCs) are potentially the most efficient and flexible fuel cells due to their ability to operate on various fuels at high temperatures.[1] The diverse array of fuels that can be fed to the anode of an SOFC include hydrogen, carbon monoxide, hydrocarbons, and alcohols.[2-4] The high operating temperature, which allows for either the direct oxidation or the internal reforming of these primary fuels, is one of the most attractive features of the SOFC. Direct use of available hydrocarbon or alcohol fuels without first reforming them to hydrogen will greatly decrease the complexity and cost of the fuel cell system.

Among potential primary fuels, a great deal of attention has recently been given to ethanol as an efficient and low-cost renewable source for hydrogen production. The estimated losses for the conversion of the energy content in sugar (glucose) to ethanol and then reacting it to yield hydrogen is below 20%.[5] A rough estimate indicates that, in principle, a perfect fuel cell can convert the hydrogen generated by 1 mol of ethanol to 350 Wh of electricity at ~$0.04/kWh.[5] Ethanol has been already produced commercially in some countries and blended with gasoline for vehicular propulsion. Usually, it corresponds only to a small fraction of the fuel used in most countries, with the notable exception of Brazil, where bioethanol (ethanol derived from biomass, in this case, sugarcane) represents ~40% of the road transportation fuel. Cost reductions associated with the scaling up of the Brazilian biomass industry have made ethanol economically competitive. Brazil has a long tradition in alternative fuels and maintains a strategic advantage in the pursuit of independent and sustainable fuel provisions due to the huge availability of ethanol, which has been estimated to be ~17 billion liters per year.[6,7]

Complete internal reforming of carbon-containing fuels in the anode of an SOFC has a number of practical issues that need further development, such as the stability of the standard Ni-based anodes and the optimization of both the exothermic electrochemical reactions and the endothermic reforming ones.[1,8] The conventional anode material used by most SOFC researchers is a yttria-stabilized zirconia (YSZ) and nickel (YSZ/Ni) cermet. This material fulfils most requirements of the anode and exhibits excellent electrochemical performance and chemical stability.[8] However, the use of hydrocarbon or alcohol fuels in an SOFC with a Ni-based anode usually results in carbon deposition and rapid cell degradation. YSZ/Ni anodes can only be directly used with such fuels if excess steam is present to ensure the complete fuel reforming and to suppress carbon deposition. Therefore, the development of anode materials for SOFCs that operate on hydrocarbons and alcohols is widely recognized to be an important technical objective.[9-11]

Several studies,[12-16] which have focused on developing carbon-resistant anodes by replacing Ni with Cu and/or ceria, indicated that a catalytic effect due to ceria is relevant. Compared to Ni, Cu is not catalytically active for carbon deposition, but it is effective as a current collector, while ceria provides catalytic activity for hydrocarbon reforming due to its mixed ionic-electronic conduction. Ceria-based materials have been pointed out as promising catalysts for ethanol oxidation.[5] However, the exact role played by mixed conductors such as ceria on the direct electrochemical oxidation of hydrocarbons is still a matter of discussion.[8]

In this context, the present study shows the direct use of ethanol as a fuel in SOFC and compares the performance of zirconia/Ni and ceria/Ni-cermet anodes in SOFCs operating with hydrogen and ethanol as fuels.

Experimental

The SOFC electrolyte substrates were prepared by uniaxial pressing of YSZ (Tosoh, Japan) powders into disks of 25 mm diameter and 1.5 mm thickness. Two sintering treatments were performed to ensure high-density (~99%) and crack-free substrates. First, the electrolyte substrates were sintered at 1500°C for 1 h with heating/cooling rates of 5°C/min. Then, the electrolytes were machined down to a thickness of ~500 μm. To minimize any mechanical stresses, the electrolyte supports were sintered at 1600°C for 1 h with the same heating/cooling rates. The $La_{0.65}Sr_{0.35}MnO_3$ cathode powders were produced by solid-state reaction and mixed with YSZ powders in a 1:1 wt % ratio.[17] Three types of anode powders were used: (*i*) a composite of 41 vol % YSZ and 59 vol % NiO, prepared by solid-state reaction and corresponding to 45 vol % Ni after NiO reduction (YSZ/45Ni);[17] (*ii*) a composite of YSZ and NiO tailored to obtain a cermet with 28 vol % Ni (YSZ/28Ni), prepared by a modified liquid mixture technique;[18] and (*iii*) a commercial composition of gadolinia doped-ceria (GDC) and NiO (Fuel Cell Materials, USA) with ~45 vol % Ni (GDC/Ni). Electrode deposition was carried out by wet spraying suspensions of either the cathode or anode powders in a solution of ethanol and polyvinylbutyral onto fixed areas of the substrate. Deposited areas of the electrodes are 0.75, 0.65, and 0.74 cm^2 for the samples YSZ/45Ni, YSZ/28Ni, and GDC/Ni, respectively. The thickness of the electrode layers were controlled by weighing after successive deposition steps until the estimated final thickness was ~50 μm. The anode/electrolyte half-cells were heat-treated at 1350°C for 1 h with heating/cooling rates of 5°C/min to avoid electrodes warping and detaching. After cathode deposition, the single

* Electrochemical Society Active Member.
z E-mail: daniel.florio@ufabc.edu.br

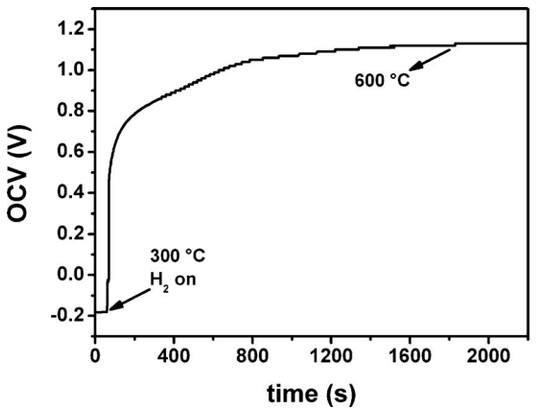

Figure 1. Typical time dependence of the open-circuit voltage of the SOFCs before, during, and after anode reduction.

cells were heat-treated at 1100°C for 1 h, with heating/cooling rates of 5°C/min. The single cells were positioned on an alumina sample chamber. Platinum meshes were used as current collector to both anode and cathode electrodes. The anode compartment was sealed with commercial cement (Aremco, USA). Further details of both single-cell fabrication and the sample chamber are found elsewhere.[17]

The reduction of NiO to Ni during single SOFC tests was achieved by flowing H_2 at 300°C during heating. The in situ anode reduction was followed by recording the open-circuit voltage (OCV). As shown in Fig. 1, when the hydrogen flux was set at 300°C, an abrupt increase of the OCV was observed from approximately −0.2 to 0.5 V. After 1800 s, the system reached 600°C and the OCV presents a stable value of ~1.15 V, which is the expected value for the Nernst potential of a fuel cell running on dry hydrogen.[19] In the case of ethanol, the fuel was delivered to the sample chamber by flowing a carrier gas (nitrogen) through ethanol in a closed Erlenmeyer flask at room temperature. The ethanol (92.8% GL) used in these experiments is commercially available in Brazil for domestic use.

The current-voltage (*I-V*) curves of single SOFCs were obtained while feeding hydrogen or ethanol to the anode and static air to the cathode. The single-cell polarization curves were collected after heating to temperatures from 600 to 900°C, and allowing the system to stabilize for 1 h at each measuring temperature. The electrochemical impedance spectroscopy (EIS) data, taken at OCV, were obtained in the 1 MHz–1 Hz frequency range with amplitude signal of 100 mV. EIS and *I-V* measurements were performed with a Solartron 1260 FRA coupled with a 1287 Electrochemical Interface. In all measurements, internal impedance associated to test chamber, leads, and connections were subtracted from the data.

Results and Discussion

The *I-V* and current-power density (*I-P*) curves of the single SOFCs with GDC/Ni, YSZ/45Ni, and YSZ/28Ni anodes, measured at 900°C, are shown in Fig. 2. The *I-V* curves are essentially linear, indicating that the main loss mechanism is related to ohmic drop from the electrical resistance of electrolyte and electrodes due to the transport of electrons and ions. The relatively low power density is likely associated with the large thickness of the electrolyte supports. No polarization losses associated with mass transfer were detected, probably due to excess fuel. *I-V* measurements performed at lower temperatures (600, 700, and 800°C) showed similar features.

Figure 2a shows *I-V* and *I-P* curves of the single cells operating with hydrogen. All samples have OCVs of ~1.2 V, and the peak power densities obtained are ~130, 60, and 50 mW/cm^2 for GDC/Ni, YSZ/45Ni, and YSZ/28Ni anodes, respectively. The experimental data evidenced the higher performance of the Ce-based anode, a

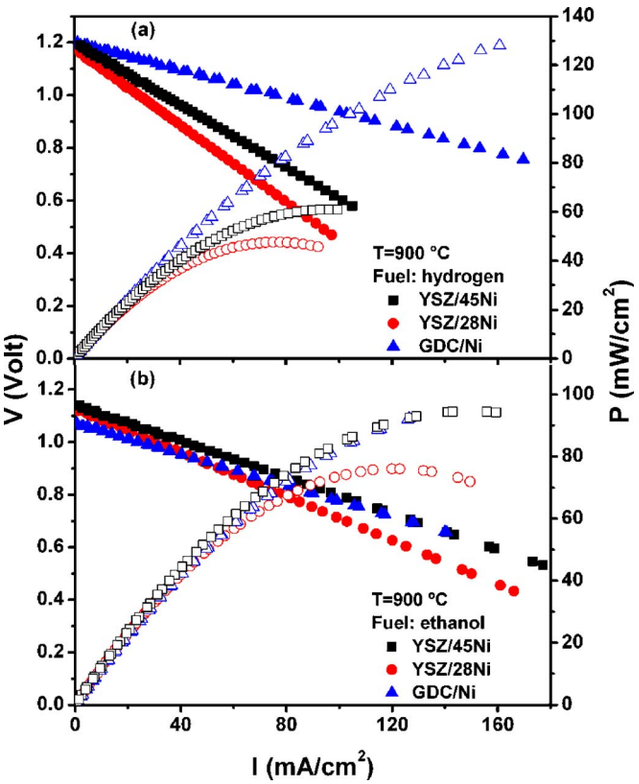

Figure 2. (Color online) Current-voltage and current-power curves of single SOFCs measured with hydrogen (a) and ethanol (b) as fuels at 900°C.

result that is likely associated with the optimized processing of the commercial material. As compared to the GDC-based anodes, cermets containing YSZ have different microstructures, as a result of the distinct preparation techniques, and lower Ni content in the case of the sample YSZ/28Ni. Previous studies demonstrated that YSZ-based cermets produced by the liquid-mixture technique display higher conductivity at relatively lower Ni concentration than do cermets produced by solid-state reaction, and the percolation threshold for the metallic phase occurred at a relatively low value (~20 vol %).[20] Those properties were attributed to the liquid-mixture process that resulted in samples with highly dispersed Ni nanoparticles.[20] The single cell using an anode produced by this technique, with 28 vol % of Ni, reaches ~80% of the maximum power density of the cell with the anode prepared by solid-state reaction with a considerably higher metal content (YSZ/45Ni). These experimental results suggest that microstructural optimization can be effective for improving anode performance. In addition, both redox tolerance and matching of the thermal expansion coefficient with YSZ are key issues that could be possibly improved with reduced Ni content at the anode, without impairing catalytic activity and electrical conductivity.[20,21]

I-V and *I-P* curves of the single SOFCs running on ethanol are shown in Fig. 2b. Using ethanol as fuel, the OCV values are lower than those measured in fuel cells operating on hydrogen. Such lower measured values for the alcohol-fueled cells are in good agreement with the theoretical OCV determined for ethanol under standard equilibrium (~1.15 V).[22] The OCV for fuel cells with anodes containing YSZ is ~1.13 V, and the one with the GDC-based cermet has a slightly lower OCV. The fuel cell using the GDC as the ceramic phase in the anode exhibited almost parallel *I-V* curves for both fuels. However, the lower OCV resulted in a significant drop of the power output from ethanol to ~40% of that obtained from hydrogen. Ethanol-fueled SOFCs have comparable peak power densi-

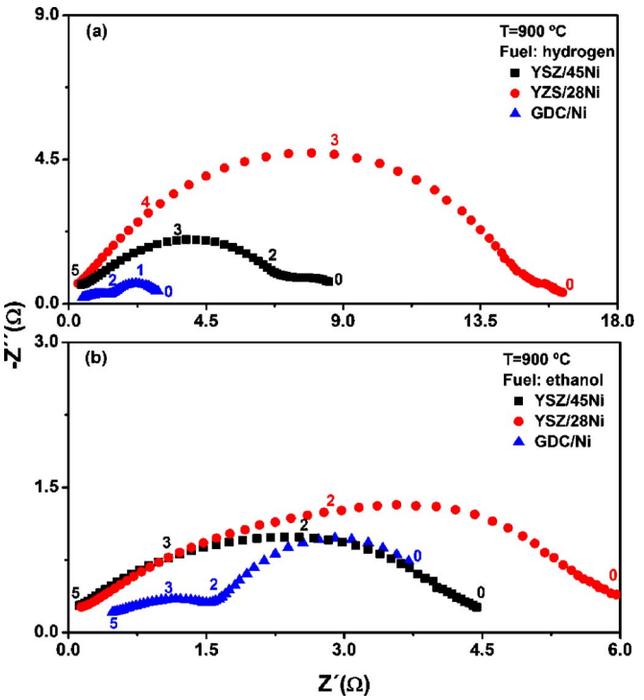

Figure 3. (Color online) Impedance diagrams of fuel cells operating on hydrogen (a) and ethanol (b) at 900°C. Numbers denote the logarithm of frequency.

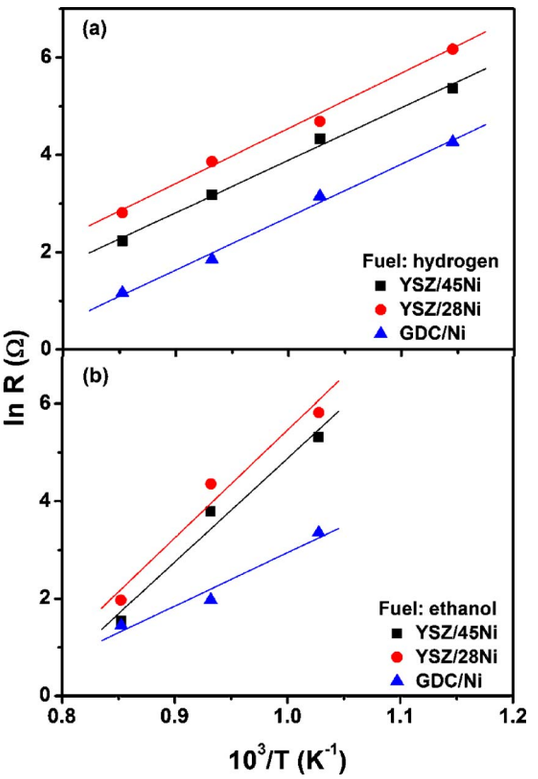

Figure 4. (Color online) Arrhenius plots of the polarization resistance of fuel cells operating on (a) hydrogen and (b) ethanol.

ties, and the *I-V* curves are significantly less dependent on the composition of the anode. The measured peak power densities obtained from ethanol are ~95 mW/cm^2 for samples with high metallic phase composition (GDC/Ni and YSZ/45Ni), and 75 mW/cm^2 for the YSZ/28Ni sample. Surprisingly, fuel cells with YSZ-based anodes delivered peak power outputs from ethanol, ~50% higher than the ones obtained with hydrogen. Such a feature was further investigated by impedance spectroscopy analysis during fuel cell operation.

Figure 3 shows the impedance spectroscopy data measured under OCV condition of the single cells running on hydrogen (Fig. 3a) and ethanol (Fig. 3b) at 900°C. In the impedance diagrams, two relaxations are clearly distinguished and related to convoluted contributions arising from both the electrolyte/electrode interfacial resistance and electrochemical reactions taking place at the electrodes.[23] Similar impedance responses have been previously reported, and the lower frequency relaxation has been associated with the anode contribution.[24,25] Indeed, by changing the fuel from hydrogen to ethanol the most significant modification observed in the impedance response occurs in the low-frequency range.

The fuel cell with GDC/Ni anode operating with ethanol exhibits higher polarization resistance than the one with hydrogen, as inferred from the low-frequency semicircle in Fig. 3. According to the phase equilibrium diagram of the Ce–O system, the transition of fluorite-type CeO_2 to Ce_3O_5 rare-earth C-type structure was attributed to the presence of ethanol at high temperature.[22,26] In the C-type structure, the ordering of oxygen vacancies, as observed by scanning tunneling microscopy and supported by theoretical calculations, is probably associated with the decrease of the ionic conductivity of doped ceria.[26] A different effect was observed when ethanol was supplied to the fuel cell with YSZ-based anodes. The experimental results indicated that carbon deposition occurs in the YSZ/Ni anodes, and as a result, the polarization resistance decreases due to the increase of the electronic conductivity from deposited carbon.[27] This enhancement of the fuel cell performance is more pronounced in the YSZ/28Ni anode, in which the reduced volume fraction of the metallic phase has limited the electronic conductivity. A similar increase of the electrical conductivity from carbon deposition in the anode was reported for Ni cermets in SOFCs operating with hydrocarbons.[9,27] Such an effect indicates that the performance of the sample YSZ/28Ni is restricted by the low electronic conductivity of the anode and that carbon formation, at least in the first few hours of fuel cell operation, was not detrimental for the SOFC using ethanol as fuel.[28] The total electrical resistance of single cells, estimated from the intercept of the impedance response with the real axis at low frequencies, is in good agreement with those calculated by the slope of *I-V* curves.

In order to further investigate the direct oxidation of ethanol, the polarization resistance, determined from the diameter of the semicircles in the impedance diagrams, was plotted as a function of the inverse of the absolute measuring temperature for fuel cells running on hydrogen and ethanol, as shown in Fig. 4.

Assuming that transport phenomena in these samples are thermally activated, the activation energies can be calculated. For fuel cells operating with hydrogen (Fig. 4a), the calculated activation energies are ~90 kJ/mol. This value is close to the expected activation energy for oxygen ion transport in YSZ and supports the pronounced ohmic polarization observed in the *I-V* curves due to the thickness of electrolyte supports (Fig. 2). The Arrhenius plots (Fig. 4b) of ethanol-fueled cells exhibit similar activation energy for the GDC/Ni anode (~90 kJ/mol), and samples with YSZ-based anodes present a much higher value. For the YSZ-based anodes, the calculated activation energy is ~177 kJ/mol, a value that was found to be in the range of the reported data for the ethanol steam-reforming reaction.[5] The distinct activation energies suggest different limiting step reactions for anodes containing GDC and YSZ when ethanol is used as a fuel. Such a feature is possibly related to both the catalytic effect of ceria, which contributes to a more effective conversion of ethanol and to the different microstructures of studied cermets.

No significant degradation effects were detected during both *I-V*

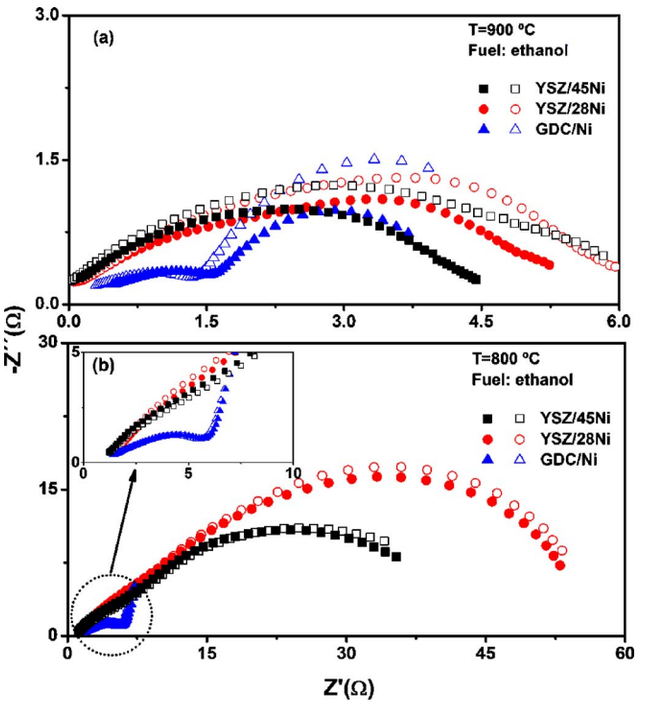

Figure 5. (Color online) Time dependence of the impedance diagrams of fuel cells operating on ethanol measured at (a) 900°C and (b) 800°C. Open and closed symbols refer to impedance data taken after 1 and 1.5 h of fuel cell operation, respectively.

and impedance measurements. However, the performance of fuel cells operating on ethanol at 900°C was not stable in the investigated conditions and, after ~1.5 h, the low-frequency branch of the impedance diagrams exhibited an increase, as shown in Fig. 5. These results confirm that continuous carbon formation resulted in cell degradation, as expected from previous investigations.[9,22,29] Nonetheless, the degradation effect was not prevented by the higher catalytic activity of the anode with doped ceria, and Ni was found to be primarily responsible for the anode deactivation, as inferred from the relatively lower increase of the nonohmic resistance of anodes with low metallic content at 900°C (Fig. 5a). The impedance data collected at 800°C (Fig. 5b) are significantly less time dependent, and the polarization resistances exhibit a much less evident increase due to carbon formation. The temperature dependence of the anode degradation is further confirmed by measurements performed at 700°C (not shown), in which no detectable increase of the polarization resistance was observed within the time length investigated. Such findings are in good agreement with previous experiments that have demonstrated an interplay between temperature and electrical current drawn from SOFCs operating on methane that can prevent carbon formation and deactivation of Ni-based anodes.[30] In that study, it has been shown that the higher is the operation temperature, the higher is the minimum current necessary to sustain the fuel cell response stable.[30]

It is important to consider that the ethanol used in the experiments here described contains insufficient water for steam reforming, and direct oxidation of the alcohol in the anode is the predominant mechanism for fuel cell operation. This process results in carbon deposition over the metallic phase of the cermet, which progressively deactivates the anodes, as inferred from the time-dependent impedance analysis. However, it was observed that, at least during the initial operation, carbon formation increased the performance of YSZ-Ni anodes by reducing the nonohmic component of the impedance diagrams. Further investigations concerning the anode microstructure, fuel cell operation conditions, and water content in the fuel are underway to optimize the experimental parameters for a stable operation of a SOFC with ethanol.

Conclusions

The direct use of ethanol as fuel in SOFCs was demonstrated in Ni cermets with either YSZ or GDC as ceramic phases. The performance of the zirconia-based cermet produced by the liquid mixture indicates that microstructural optimization can be effective for improving anode properties. Ethanol-fueled cells have comparable peak power densities irrespectively of the preparation method and composition of the anode. The experimental data show that the catalytic activity of the ceramic phase, as in the case of doped ceria, is insufficient to stabilize the anode. The deactivation of the anodes of fuel cells operating with ethanol was found to be more pronounced at high temperatures (>800°C) and for anodes with high content of Ni. The experimental results provide evidence for the importance of an appropriate combination of fuel, operating conditions, and anode materials in designing SOFCs for direct operation using ethanol as fuel.

Acknowledgments

The authors thank Fundação de Amparo à Pesquisa do Estado de São Paulo, FAPESP (proc. no. 05/53241-9). R.M., E.N.S.M., and F.C.F. acknowledge CNPq (proc. no. 306496/88, 301820/2004-0, and 301661/2004-9).

Universidade Federal do ABC assisted in meeting the publication costs of this article.

References

1. N. Q. Minh, *Solid State Ionics*, **174**, 271 (2004).
2. K. Sasaki, K. Watanabe, K. Shiosaki, K. Susuki, and Y. Teraoka, *J. Electroceram.*, **13**, 669 (2004).
3. B. C. H. Steele and A. Heinzel, *Nature (London)*, **414**, 345 (2001).
4. R. Craciun, S. Park, R. J. Gorte, J. M. Vohs, C. Wang, and W. L. Worrell, *J. Electrochem. Soc.*, **144**, 4019 (1999).
5. G. A. Deluga, J. R. Salge, L. D. Schmidt, and X. E. Verykios, *Science*, **103**, 993 (2004).
6. J. Goldenberg, *Science*, **315**, 808 (2007).
7. A. Bauen, *J. Power Sources*, **157**, 893 (2006).
8. M. Mogensen and K. Kammer, *Annu. Rev. Mater. Res.*, **33**, 321 (2003).
9. B. Huang, S. R. Wang, R. Z. Liu, and T. L. Wen, *J. Power Sources*, **167**, 288 (2007).
10. S. P. Jiang and S. H. Chan, *J. Mater. Sci.*, **39**, 4405 (2004).
11. B. C. H. Steele, *Solid State Ionics*, **86-88**, 1223 (1996).
12. H. Kim, C. da Rosa, M. Boaro, J. M. Vohs, and R. J. Gorte, *J. Am. Ceram. Soc.*, **85**, 1473 (2002).
13. S. Park, R. J. Gorte, and J. M. Vohs, *J. Electrochem. Soc.*, **148**, 443 (2001).
14. S. Park, J. M. Vohs, and R. J. Gorte, *Nature (London)*, **404**, 265 (2000).
15. R. J. Gorte, S. Park, J. M. Vohs, and C. Wang, *Adv. Mater. (Weinheim, Ger.)*, **12**, 1465 (2000).
16. S. Park, R. Cracium, J. M. Vohs, and R. J. Gorte, *J. Electrochem. Soc.*, **146**, 3603 (1999).
17. R. Muccillo, E. N. S. Muccillo, F. C. Fonseca, Y. V. França, T. C. Porfirio, D. Z. de Florio, M. A. C. Berton, and C. M. Garcia, *J. Power Sources*, **156**, 455 (2006).
18. V. Esposito, D. Z. de Florio, F. C. Fonseca, E. N. S. Muccillo, R. Muccillo, and E. Traversa, *J. Eur. Ceram. Soc.*, **25**, 2637 (2005).
19. N. Q. Minh, *J. Am. Ceram. Soc.*, **76**, 563 (1993).
20. F. C. Fonseca, D. Z. de Florio, V. Esposito, E. Traversa, E. N. S. Muccillo, and R. Muccillo, *J. Electrochem. Soc.*, **153**, 354 (2006).
21. D. Waldbillig, A. Wood, and D. G. Ivey, *J. Electrochem. Soc.*, **154**, 133 (2007).
22. T. Iida, M. Kawano, T. Matsui, R. Kikuchi, and K. Eguchi, *J. Electrochem. Soc.*, **154**, B234 (2007).
23. S. P. Jiang, J. G. Love, and Y. Ramprakash, *J. Power Sources*, **110**, 201 (2002).
24. B. W. Chung, C. N. Chervin, J. J. Haslam, A.-Q. Pham, and R. S. Glass, *J. Electrochem. Soc.*, **152**, 265 (2005).
25. T. Tsai and S. A. Barnett, *Solid State Ionics*, **93**, 207 (1997).
26. C. T. Campbell and C. H. F. Peden, *Science*, **309**, 713 (2005).
27. S. McIntosh, H. He, S.-I. Lee, O. Costa-Nunes, V. V. Krishnan, J. M. Vohs, and R. J. Gorte, *J. Electrochem. Soc.*, **151**, 604 (2004).
28. T. Kim, K. Ahn, J. M. Vohs, and R. J. Gorte, *J. Power Sources*, **164**, 42 (2007).
29. A. S. Ferlauto, D. Z. de Florio, F. C. Fonseca, V. Esposito, R. Muccillo, E. Traversa, and L. O. Ladeira, *Appl. Phys. A: Mater. Sci. Process.*, **84**, 271 (2006).
30. Y. Lin, Z. Zhan, J. Liu, and S. A. Barnett, *Solid State Ionics*, **176**, 1827 (2005).